2006 INTERNATIONAL COALBED METHANE SYMPOSIUM

0602

DIFFERENTIAL SWELLING AND PERMEABILITY CHANGE OF COAL IN RESPONSE TO CO_2 INJECTION FOR ENHANCED COALBED METHANE

Saikat Mazumder, Nikolai Siemons and Karl Heinz Wolf
Department of Geotechnology, Delft University of Technology, The Netherlands

ABSTRACT

The matrix volume of coal swells when CO_2 / CH_4 adsorb on its coal structure. In coalbed gas reservoirs, matrix swelling could cause the fracture aperture width to decrease, causing a considerable reduction in permeability. On a unit concentration basis, CO_2 causes greater degree of coal matrix swelling compared to CH_4. Much of this difference is attributable to the differing sorption capacity that coal has towards carbon dioxide and methane. This condition in a coal reservoir would lead to differential swelling. Differential swelling will have consequences in terms of porosity / permeability loss, with serious implication for the performance and implementation of carbon sequestration projects.

Coal can be understood as a macromolecular cross linked polymeric structure. An experimental effort has been made to measure the differential swelling effect of CO_2 / CH_4 on this macromolecular structure and to theoretically translate that effect in terms of porosity and permeability. A unique feature of this work is that, real time permeability measurements were done to see the true effect of differential strain from CH_4 saturated coal core flooding experiments.

INTRODUCTION

Coal matrix is heterogeneous and is characterized by three different porosity systems - micropores, mesopores and macropores. The macropores are the cleats, which are sub-vertically oriented to the bedding plane in coal. The cleat system consists of the face cleats, continuous throughout the reservoir, and butt cleats, which are discontinuous and terminates against the face cleat.

Permeability of coal is recognized as the most important parameter for gas and fluid transport through the seam. Cleat permeability is considered to be primarily controlled by the prevailing effective horizontal stress under uniaxial strain reservoir conditions.

Various ECBM technologies have been proposed to improve the coalbed methane recovery. One of the methods is based on the principle of inert gas stripping, where a low sorbing or non sorbing gas like N_2 or H_2 is injected. Since sorption of CH_4 depends on the partial pressures, the process of stripping reduces the partial pressures of methane in the free gas phase and favoring desorption of methane from the adsorbed phase [17, 1]. As an alternative, injected CO_2, being preferentially sorbed in coal competes with methane for the same sorption site. It enhances methane production both by reducing the partial pressure of CH_4 and by preferential sorption. Laboratory experiment among others, by Kross et al. [9] suggests that for every methane molecule produced about two molecules of CO_2 are sequestered. Furthermore, this exchange ratio could be higher at pressures corresponding to supercritical CO_2 conditions [6]. Moreover this technique has its associated problem in the name of differential swelling.

Extensive lab data in literature reveals that CO_2 causes a greater degree of coal matrix swelling compared to methane, even when measured on a unit concentration basis [11, 2]. This effect has been emphasized in the work

of Pekot and Reeves [15]. CO_2 adsorption causes more strain and swelling than CH_4, since it is adsorbed in higher concentration. Differential swelling is caused by an excess strain produced by CO_2 over CH_4 on a unit concentration basis. This suggests that the physical change introduced in the macromolecular network structure of coal, as a result of CO_2 dissolution, is more pronounced as compared to CH_4. This observed difference in the swelling capacity is termed as differential swelling.

The chemical reasoning behind the process is explained in polymer sciences, where coal is compared to glassy polymeric systems. Reucroft and Patel [18] have looked into the thermodynamic swelling theories for a cross linked macromolecular network structure. This theory predicts that maximum swelling occurs when the solubility parameter of a gas molecule (δ_{gas}) is equal or close to the solubility parameter of the macromolecular network (δ_{coal}) [12]. The solubility parameter (δ) is defined in terms of molar enthalpy of vaporization (H_v) and the molar volume (V).

$$\delta = \sqrt{\left(\frac{H_v - RT}{V}\right)} \tag{1}$$

The solubility parameter of CO_2 ($\delta_{CO_2} \approx 6.1 cal^{0.5} cm^{-1.5}$) being closer to the solubility parameter of coal ($\delta_{coal} \approx 10 cal^{0.5} cm^{-1.5}$) yields higher swelling as compared to CH_4 and N_2 on a unit concentration basis. The solubility parameter of organic solvents like pyridine and acetone are even higher than that of CO_2, thus yielding higher swelling of coal.

Laxminarayana et al. [2] derives a linear relationship between volumetric strain and gas concentration for CO_2, CH_4, N_2 and H_2S. From his experiments on four different coal samples at any unit gas concentration, the volumetric strain for CO_2 was at least 1.5 times higher than from methane.

Differential swelling as a result of CO_2 injection can cause profound changes in fracture porosity and permeability with significant implication for enhanced methane recovery. Permeability is coal change due to two reasons [5], a change in the effective horizontal stress and a change caused due to a differential matrix swelling / shrinkage.

The effect of matrix swelling and shrinkage on cleat permeability of coal samples has been investigated by a number of researchers [22, 3, 5, 7, 19, 20, 14, 4, 21, 2]. All proposed models, almost invariably has two terms to define the porosity change, a term to account for the pressure dependent nature of the coal porosity, while a second term which accounts for porosity changes due to matrix shrinkage and swelling. Pekot and Reeves [15] and Laxminarayana et al. [2] incorporated the effect of differential swelling on fracture porosity in coal. Recent effort by Mavor et al. [13] to model the effect of differential swelling on secondary porosity and permeability of coal is quite commendable. Most of the experimental data presented here can be used to calibrate the model.

This paper presents an experimental effort to measure the effect of differential swelling on coal permeability, using the axial strain measurements on a coal core sample. A linear variable differential transformer (LVDT) has been used to measure the axial strain. The paper also presents a model, which describes the porosity change due to differential swelling as a function of the change in partial pressures using pressure - time relations.

EQUIPMENT DESIGN

The equipment was designed according to the primary objective of the experiments. Hence, it is necessary to explain the specific objectives:

(i) To determine the differential swelling as a result of CO_2 injection in an initially methane saturated coal core.

(ii) To determine the sweep efficiency of CO_2 as a function of the initial methane saturation at a constant mean pore pressure and constant P_{eff} .

(iii) To estimate and to establish the dependence of permeability on the differential swelling of coal i.e. the effect on permeability due to change in the partial pressures of CH_4 and CO_2 in the free gas phase. The effective stress

(P_{eff}), the pressure difference ($P_{injection} - P_{production}$), the mean pore pressure (P_{mean}) and the injection rate are kept constant over the course of the flooding experiment.

The uniqueness of these experiments, using large cores, makes the design of the setup complex. The reasons to use large core samples are as follows; heterogeneity of the coal matrix is sufficiently guaranteed and the dual porosity nature of coal is retained. Taking this into consideration a high-pressure core flooding setup was constructed. The schematic of the setup is shown in Fig. 1. The pressure cell is 1m in length and can reach a maximum confining oil pressure of 50 MPa and a temperature of 420 K. The confining pressure was applied on the coal core, inside a rubber sleeve. To prevent the gas from diffusing through the rubber sleeve, 0.2 mm lead foil was wrapped around the coal core. To simulate downhole conditions the temperature in the pressure cell was maintained at around 45^0C. The pressure cell can handle samples up to a diameter of 120 mm and a core length of 500 mm. The length of the core varied from sample to sample. The dimensions of the coal core used in our experiments are provided in Table 2. To avoid mechanical end effects on the core permeability, two sieperm plates are fixed at both ends of the core. These sieperm plates have a porosity of 33% and a permeability of 10^{-13} m^2. The injection and production tubing's were attached to the end plates.

The measurement of sorption related strain of coal is subject to analytical difficulties. To avoid longer and tedious sample preparation process a simple mechanical micrometer (LVDT) was used to measure the axial strain in the coal core. The cores were drilled parallel to the bedding plane, thus ensuring that the axial strain measured was bedding parallel.

The high pressure cell consists of the following peripheral devices. All description of peripheral devices is in order of the flow direction.

- An ISCO TM plunger pump connected to a bottle of the required gas to be injected. The ISCO plunger pump injects CO_2 into the coal core at a constant injection rate. The average of the injection and production pressure was taken as the pressure over the core and used for the calculation of the Darcy permeability. At the production end, a backpressure valve controlled the flow out. A constant pressure difference ($P_{injection} - P_{production}$) was necessary to measure the permeability consistently during the experiment.

- A linear variable displacement transformer (LVDT) measured the axial changes of the core dimension (μ-strains) throughout the course of the experiment. The strain measurements were stored, through a data acquisition system, on a computer.

- Gas analyzer (GC). The gas chromatograph used for analyzing the product gas was an Agilent TM 3000 micro GC with a TCD (Thermal Conductivity Detector). This micro GC has two types of columns, a Molsieve column and a Poraplot U column. For data acquisition and analysis the software, "Agilent Cerity TM" was used. The carrier gas used for measurements was helium. The molsieve column allowed measuring hydrogen, oxygen, nitrogen, methane and carbon monoxide. The poraplot U column measures carbon dioxide, ethylene, ethane, acetylene and sulfur dioxide separately. For accuracy both columns were cleaned for at least 12 hrs on a weekly basis. The micro GC was calibrated repeatedly with the Universal Gas Calibration Standard. Every gas component had its own reference factor, mainly dependent on it's thermal conductivity. This type of calibration is referred to as single level calibration. The calibration procedure was done under the same conditions as used in the experiment. The calibration peak area of a component defines a reference area corresponding to a reference concentration. The concentration of a measured component is given by the ratio of the peak areas times the reference concentration. The micro GC was connected directly to the outgoing flow vent of the autoclave and automatically sampled. The actual volume analyzed is estimated to be +/-0.853µL out of the 2.39±0.1ml used to flush the sample loop. To avoid damage of the micro GC, a silica gel bottle was used to remove all the moisture from the produce gas.

- Flow analyzer. At the end of the line an analog flow analyzer, i.e. an Acataris TM water clock measured the remaining gases leaving the system. This type of analog flow analyzers runs at an accuracy of 0.1 ml/hr. The flow rate was camera recorded and afterward used for mass balance calculations and permeability measurements.

- Operational panel, safety device and data acquisition system. The operation panel, the data-acquisition system and safety devices were installed in the control room. During the test, two thermocouples were used to measure temperatures above and below the core inside the pressure cell. In addition, the (differential) pressure, tube / sample expansion and flows were registered every 30 seconds.

SAMPLE DESCRIPTION

The unique properties of coal put constraints on preparation and preservation of coal samples. When exposed to air, the effect of drying and weathering would result in the alteration of structure of coal and development of induced fractures. The permeability and porosity values of such samples may be significantly different from the samples that are well preserved. The cores were drilled from big blocks of coal. Coal samples used for these experiments were kept in water to avoid contact with air and drying. Once drilled the cores were put in sealed polythene bags and cooled to prevent oxidation or loss of moisture. All the coal cores were drilled parallel to the bedding plane.

The samples used for these experiments were from the Beringen coal mines (Beringen 770) in Belgium, the Silezia coalfield in Poland (Silezia 315 II) and the Tupton coalfields in UK. The details of the samples are shown in Table 1. Five different flooding experiments were conducted on coal cores drilled from the samples mentioned above. The details of the coal cores and their experimental conditions are in Table 2.

DIFFERENTIAL SWELLING EXPERIMENTS AND PERMEABILITY MEASUREMENTS

Experimental procedure

The differing sorption capacities that a coal exhibits for different gases makes it important to study the effects of CH_4 and CO_2 on the strain, porosity and permeability of coal during the enhanced recovery process. The axial strain measurements give an estimate of the differential swelling of coal. The experiments start with a complex procedure of mounting the coal core sample in a rubber sleeve and building it in the high-pressure cell; leak free. A detailed procedure for volume measurement was then followed. The volume measurements were conducted with and without the sample built in the pressure cell. The tubing volume in the whole setup is quite considerable. The effect of this dead volume is seen in the results and has been discussed later in this section. All mass balance calculations for CH_4 and CO_2 do take care of the free and the adsorbed volumes separately.

At the end of the volume measurement the sample cell was connected to a vacuum pump, for at least a week, to eliminate any form of residual gas or moisture. During this process temperature was kept constant. Thereafter the coal was filled with methane in increasing pressure cycles, till the required pore pressure was achieved. After each injection cycle the methane was allowed to sorb onto the coal matrix until equilibrium was reached. To meet sub-surface conditions, the difference between the annular pressure and the pore pressure was usually kept at ratios in between 2:1 up to 5:3. The volume of injected methane was measured with a mass flow meter. Thereafter the tubing system and the pump were brought again to the same pressure and temperature conditions as the methane filled sample. More methane will adsorb and again time was needed for this methane to reach a new equilibrium pressure. In the following injection cycle the pump was filled with CO_2 and injection was started at a certain rate. Keeping a constant pressure gradient over the whole core with the help of a backpressure valve, the system was allowed to produce alongside injection. The gas analyzer determines the relative amount of CH_4 and CO_2 in the product gas. The gas chromatographic measurements were assumed to be representative of the change in molar concentrations of CH_4 and CO_2 in the free phase. This is partly true, but is a reasonable assumption to understand the permeability variation. The moisture if any was separated using silica gel bottle connected to a balance. During the tests the recorded data serve as an iterative feedback to rule out their influence in the interpretation afterwards.

Five different differential sorption experiments were conducted (Table 2). The experiments range from sub-critical to super-critical CO_2 conditions. Experiments I and II were conducted on the Beringen 770 sample from Belgium. Both experiments were conducted on dry coal samples. Experiments III and IV were conducted on the Silezia 315 II sample from Poland. Experiment III was carried out on a moisture equilibrated coal while experiment IV was carried out on a dry coal. The effect of moisture is evident from the low sweep efficiency. Experiment V was performed on a dry coal sample from UK (Tupton) at a very high mean pore pressure of 23 MPa.

The permeability of the coal varies due to a combined effect posed by the process of differential sorption. It varies due to shrinkage, while methane is being desorbed and due to swelling, while carbon dioxide is being injected. The effect of swelling due to CO_2 sorption is more profound, thus resulting in an excess volumetric strain. The test procedure to measure permeability change during the differential sorption experiments, involved the simulataneous injection of CO_2 and production of the mixed gas under steady pressure conditions. The injection of CO_2 was done with the ISCO pump at a constant rate. A mass flow meter was used to measure the flow on the production end. To keep the downstream peressure constant and to create a pressure gradient, a back pressure

valve was used. Because gas pressure varied across the sample, the average of the two end gas pressures was used in the calculation of the effective stress. As permeability is a function of the effective stress, it was kept constant during the experiment. The equation below was used to calculate the core permeability [5].

$$k = (1.013x10^{13})\frac{2qP_oL\mu}{A(P_i^2 - P_o^2)} \quad (2)$$

The flow measurements for a particular permeability step were only used when all equilibrium conditions were satisfied. The differential swelling corresponding to the differential gas sorption is controlled by the change in the partial pressures of the individual components. Assuming Darcy's flow to be the primary means of gas transport through the cleats, ample care was taken to see that the adsorbed gas is in dynamic equilibrium with the free gas phase, although at times this was very difficult to attain. The difference between the injection and the production pressure was kept constant during the flow measurements.

Results and discussion

Differential swelling from all five experiments here, are reported as measured linear strain in the axial direction of the core and not as volumetric strain. All the differential strain measurements are shown in the Figs. 2, 5, 8, 11 and 14. There was no need to correct the strain measurements for mechanical compliance as the injection and production scheme was at constant pore pressure and effective stress. In all five experiments, as can be seen from the plots, the coal does not start to swell right at the onset of CO_2 injection. The delay in the strain response is because of the fact that the injected CO_2 had to displace the tubing volume preceding the core, before it reached the coal.

The sweep efficiencies and the molar concentration changes have been plotted against the displaced volume for all five experiments in Figs. 3, 6, 9, 12 and 15. Sweep efficiencies of all four dry experiments ranged between 60 to 90 % of the methane initially in place. Sweep efficiency and displaced volume are defined as follows:

$$Sweep\ effeciency\ (\%) = \frac{moles\ of\ CH_4\ produced}{moles\ of\ CH_4\ initially\ in\ place} x100 \quad (3)$$

$$Displaced\ volume = \frac{moles\ of\ CO_2\ injected}{moles\ of\ CH_4\ initially\ in\ place} \quad (4)$$

The results of experiment I and II have been cited in Table 3. The experimental conditions prior to the start of CO_2 injection have been shown in Table 2. Figs. 3 and 6 show migration history of CH_4 and CO_2 during the course of the experiment. Both the experiments were conducted at a temperature of 45^0C. While the injection rate for experiment I was 6 ml /h, that of experiment II was set as low as 0.7 ml /h. Pressure and temperature conditions for both CH_4 and CO_2 were sub-critical in case of experiment I, but were super-critical for experiment II. As can be seen from the migration data (Figs. 3 and 6) the injection pressure does not have a big influence on the methane recovery. Diffusion is much faster under sub-critical conditions as compared to super-critical conditions. CO_2 is five times denser than CH_4 under super-critical conditions. The coal core used in experiment I is twice as long as that of experiment II (Table 2). As can be seen from Table 3, the breakthrough time for experiment I is almost two times faster than experiment II. Thus with an injection rate of 6 ml /h the sub-critical CO_2 is traveling two times the distance in half the time as compared to an injection rate of 0.7 ml /h . Also at breakthrough (1% CO_2), almost all the free methane in the system have been produced whereas only half the free volume of methane have been produced for the second case. From the displaced volume data it is evident that in terms of simple methane recovery, at 90% of product CO_2 concentration, experiment I might look more efficient as it takes almost five times less time to remove almost equal concentration pf CH_4 from the system. It can be seen that for better exchange and storage of CO_2, the residence time for CO_2 in the coal has to be longer. Diffusion is more pronounced in experiment II than in experiment I where the injected CO_2 races through the core to get produced.

The results from experiment III and IV can be used to compare the influence of water on the CO_2-CH_4 exchange process in the coal. The experimental conditions for these experiments have been shown in Table 2. Both the experiments were conducted on the same coal sample. Experiment II was conducted on a wet coal core where there was excess water present in the fracture system of the coal. No free water was present in the relatively dry experiment IV. The comparative results of the experiments have been summarized in Table 4. The wet experiment was conducted for a much longer duration as compared to the dry one. It is seen that only 34% of the CH_4 in place was produced at the end of the wet experiment, whereas almost 79% of the CH_4 in place was

produced from the dry experiment. An estimate shows that, apart from the free methane that was produced, only 3% of the adsorbed methane was produced from the wet experiment as compared to 50% from the dry experiment. From Table 4 it is seen that there is no considerable difference in the breakthrough time for both the experiment. A slightly faster breakthrough for the wet experiment can be possibly because of the fact, that the dissolved CO_2 might get produced along with the water which is forced out of the fracture space. Looking at the sweep efficiencies at different times from Table 4, the methane recovery for the relatively dry experiment is way too high as compared to the wet experiment. The CO_2 storage capacity doesn't differ much. This is also an indication towards the fact that CO_2 occupies different sorption sites than CH_4. The CO_2 and CH_4 migration data for both the experiments have been shown in Figs. 6 and 9.

With the injection of CO_2 the partial pressure of CH_4 in the free phase decreased, inducing the production of methane. Whether or not CO_2 was preferentially replacing CH_4 was not clear, but from the CO_2 mass balance and from the differential swelling it was evident that the solubility of CO_2 in coal is more pronounced than that for CH_4. The term solubility has been used considering that swelling is referred to as an increase in the volume occupied by the coal as a result of the viscoelastic relaxation of its highly crosslinked macromolecular network [10]. Moreover all four dry experiments indicate that the amount of CH_4 desorbed is marginally greater than the desorption resulting from the reduction in partial pressures of methane. This was not true for the wet experiment. Consequently, under dry conditions, the incremental methane produced, is likely due to the preferential desorption of methane in the presence of CO_2. Since differential sorption is a fact as can be seen from the differential strain data, it can be concluded that CO_2 causes more strain on a unit concentration basis.

Binary gas sorption experiments conducted by Prusty et al. [16] and Laxminarayana [2] are different from these experiments. In those experiments a static equilibrium was attained before each measurement was conducted. In the experiments reported in this article a dynamic setup is presented, which is comparing a field situation in a better way.

The results of the permeability measurements in the laboratory are shown in the Figs. 4, 7, 10 and 13. Uncertainty principle has been used to determine the possible random errors in the experimental permeability measurements. A detail of the error analysis procedure is explained in Appendix A. Under stress, the Belgian and the Polish coal samples have low initial permeability's. All five experiments were conducted at constant mean pore pressure and at constant effective stress conditions. Since the coal core was free to swell inside the pressure cell (unconstrained swelling), the measured permeability increase correspond to an increase in the differential strain in coal. This whole process of free swelling in the laboratory in comparison to constrained swelling in the field is analogous to thermal expansion [21]. A hollow steel pipe when subjected to thermal expansion encounters an increase in its free volume, which is analogous to an increase in the cleat porosity with increasing differential swelling in our case.

From the experimental results (Figs. 4, 7, 10 and 13), changes in cleat porosity was calculated. The increase in coal cleat volume due to differential swelling is considered to be equal to the decrease in cleat porosity under field conditions with constrained swelling. This assumption is valid when the total volume of coal (matrix and cleats) remains constant with injection of CO_2.

Using the experimentally determined permeability measurements under unconstrained conditions (Figs. 4, 7, 10 and 13) and assuming that permeability varies with porosity as follows,

$$\frac{k}{k_0} = \left(\frac{\phi}{\phi_0}\right)^3 \frac{(1-\phi_0)^2}{(1-\phi)^2} \tag{5}$$

changes in cleat porosity were calculated. The increase in coal cleat porosity due to unconstrained swelling is considered to be equal to the decrease in cleat porosity under field conditions with constrained swelling. This assumption is valid when the total volume of coal (matrix and cleats) remains constant with injection of CO_2. With the decrease in cleat porosity calculated, the permeability variation under constrained condition was determined. Although significant advances have been made, it is still difficult to measure cleat porosity accurately because of the very small volume of cleats in solid coal. For a simple model like the above, any value for the initial cleat porosity returns the same estimate for the change in permeability with differential swelling of coal. The resulting variations in permeability alongside differential strain for all five experiments are shown in Figs. 5, 8, 11 and 14. For all initial porosity cases, the permeability variation corresponding to differential swelling is dependent on the differential swelling capacities of coal, for each gas, on a unit of concentration basis. Under laboratory conditions

the negative permeability can be explained as the flow, which takes place through the coal matrix and can no longer be considered as a fracture or cleat flow. Model generated negative permeability and porosity lacks any physical meaning. But, this retains the essence of the swelling induced injectivity problem. This has also been reported by Zutshi and Harpalani [24] with a matchstick model. Negative permeability and negative porosity values indicate near zero porosity and permeability at those pressures. This problem can be anticipated at field scale injection projects in low permeability coal. Thus injecting under a near zero permeability condition results into very high bottom hole pressures, which exceeds fracture breakdown limit resulting in propagation of uncontrolled fractures.

CONCLUSIONS

Experiments conducted to measure the differential swelling of coal were successful. Differential strain develops as a result of the excess strain caused by the dissolution of CO_2 in coal when compared with CH_4 on a unit concentration basis. Linear strains in the order of 0.0015 to 0.006 are measured in that respect.

The effect of the differential swelling on the fracture porosity and permeability of coal has been experimentally determined. The uncertainty in the measurements has been determined and shows that the pressure gradient over the core has the greatest influence on the error measurements.

Thus differential swelling is a condition that has been measured and observed in the laboratory, where it carries a different degree of permeability change on a unit concentration basis. Work needs to be done to understand the chemical behavior of coal, CH_4 and CO_2 in the process of differential swelling.

APPENDIX A - ERROR ANALYSIS

The uncertainty principle was used to estimate the experimental error in measuring the permeability. The principle is based on the concept of calculating the uncertainty in the final value of the calculated parameter from the uncertainties of each measured variables [8, 23]. The effects of each measured variables on the final calculated variable value is derived from the concept of propagation of errors. The concept is best explained by the following example:

For evaluation of the uncertainty in the value of parameter *R*, where *R* is a function of independent variables (x_i), i.e.:

$$R = R(x_1, x_2, x_3, \ldots\ldots\ldots\ldots x_n) \tag{A-1}$$

where if U_R denotes the uncertainty in the result *R* and, U_i is the uncertainty in each variable x_i, then the uncertainty U_R is given by

$$U_R = \left[\left(\frac{\partial R}{\partial x_1} U_1 \right)^2 + \left(\frac{\partial R}{\partial x_2} U_2 \right)^2 + \ldots\ldots\ldots\ldots + \left(\frac{\partial R}{\partial x_n} U_n \right)^2 \right]^{\frac{1}{2}} \tag{A-2}$$

Applying this concept for our case and starting with the permeability equation (Eq. 2), the measured independent variables are: q , L , P_o and P_i. All the other terms have been put as a constant in the term θ.

$$k = \frac{\theta q L P_o}{P_i^2 - P_o^2} \tag{A-3}$$

Taking partial derivative of k with respect to the above mentioned independent variables, the uncertainty in permeability is then derived as

$$(\partial k) = \sqrt{\left[\begin{array}{l}\left(\frac{\theta L P_o}{P_i^2 - P_o^2}\partial q\right)^2 + \left(\frac{\theta q P_o}{P_i^2 - P_o^2}\partial L\right)^2 + \\ \left(\frac{\theta q L\,(P_i^2 + P_o^2)}{(P_i^2 - P_o^2)^2}\partial P_o\right)^2 + \\ \left(\frac{-2\theta q L P_i P_o}{(P_i^2 - P_o^2)^2}\partial P_i\right)^2\end{array}\right]} \tag{A-4}$$

All error measurements of the experimental permeability data have been presented as +/- error bars. This is shown in the figs. 4, 7, 10 and 13. More than 95 % of the random error in the permeability measurements was introduced by the uncertainty in the injection and the production pressures.

APPENDIX B – PERMEABILITY CHANGE MODEL FOR DIFFERENTIAL SWELLING OF COAL (SATURATED RESERVOIRS)

The pressure dependent nature of coal porosity has been rightly modeled by most previous researchers. Thus the focus has been to model the porosity change due to differential swelling as a function of the change in partial pressures using extended Langmuir formulation to model the differential strain.

For isothermal coalbeds, the uniaxial strain caused by coal matrix swelling upon gas adsorption is analogous to the strain due to the temperature changes for thermo-poroelastic medium [14]. The derivation makes an analogy between thermal expansion and matrix swelling associated with differential sorption in coalbeds. Stress strain relationship for a thermoplastic porous media has been picked up from available literature [21]. In a non-isothermal body, if the temperature increases the fabric swells, leading to a decrease in the porous medium porosity. This is directly analogous to matrix swelling in coal, where the porosity decreases as a result of differential sorption of a binary gas mixture.

$$-d\phi = -\frac{1}{M}dp + \left[\frac{1}{3}\left(\frac{1+\nu}{1-\nu}\right) + f - 1\right]\gamma dp - \left[\frac{1}{3}\left(\frac{1+\nu}{1-\nu}\right) - 1\right]\alpha dT \tag{B-1}$$

In the original Palmer and Mansoori[13] formulation as shown above the first series of terms to the right hand side of the equation account for the pressure dependent nature of the coal porosity, while the second term accounts for the porosity change due to matrix shrinkage (in primary depletion). The second term is of interest and is open for improvement to incorporate the aspect of differential swelling. Replacing the thermal expansion term (*dT*) in the equation by an analogous swelling term we get

$$d\phi = \left[\frac{1}{3}\left(\frac{1+\nu}{1-\nu}\right) - 1\right]\frac{d}{dp}\left(\frac{\varepsilon_i \beta_i X_i p + \varepsilon_j \beta_j X_j p}{1 + \beta_i X_i p + \beta_j X_j p}\right)dp \tag{B-2}$$

Where

$$\beta_{i,j} = \frac{1}{P_{\Psi_{i,j}}} \tag{B-3}$$

$$X_{i,j} p = p_{i,j} \tag{B-4}$$

The above equation has been formulated by drawing a direct analogy of differential swelling to extended Langmuir equation for multi component gas sorption. Such an analogy comes with some assumptions which are as follows,

(i) The adsorbed gas is in equilibrium with the free gas phase in the fractures, this is true if the gas transport through the cleats is controlled by Darcy's flow.

(ii) The differential swelling corresponding to the differential gas sorption is controlled by the change in the partial pressures ($p_{i,j}$) of the individual components.

Since an enhanced recovery project will only be taken up after primary depletion, such an injection production system would preferably be operated at a constant reservoir pressure. Any increase or decrease in the reservoir pressure would mean the addition of an extra porosity change term to accommodate the change in the effective horizontal stress normal to the cleat.

Eq. (B-2) can be simplified by making the following replacements,

$$\alpha = \left[\frac{1}{3}\left(\frac{1+\nu}{1-\nu}\right)-1\right] \tag{B-5}$$

$$a = \beta_i X_i;\ b = \beta_j X_j;\ x = \varepsilon_i;\ y = \varepsilon_j$$

Integrating Eq. (B-2) we get,

$$\phi = \alpha\left(\frac{1}{a+b}(ax+by)+\frac{-ax-by}{a+b+2abp+a^2p+b^2p}\right) \tag{B-6}$$

For an initially methane saturated reservoir, the mole fraction of CO_2 is zero. Thus,

$$\phi-\phi_0 = \alpha\left(\frac{ax+by}{a+b}-\frac{ax+by}{a+b+2abp+a^2p+b^2p}\right)-\alpha\left(\frac{axp_0}{1+ap_0}\right) \tag{B-7}$$

$$\frac{\phi}{\phi_0} = 1+\frac{\alpha}{\phi_0}\left(\frac{ax+by}{a+b}-\frac{ax+by}{a+b+2abp+a^2p+b^2p}-\frac{axp_0}{1+ap_0}\right) \tag{B-8}$$

Substituting the corresponding values of α , a , b , x and y we get,

$$\frac{\phi}{\phi_0} = 1+\frac{1}{\phi_0}\left[\frac{1}{3}\left(\frac{1+\nu}{1-\nu}\right)-1\right]\left(\begin{array}{l}\dfrac{\beta_i X_i\varepsilon_i+\beta_j X_j\varepsilon_j}{\beta_i X_i+\beta_j X_j}- \\ \dfrac{\beta_i X_i\varepsilon_i+\beta_j X_j\varepsilon_j}{\beta_i X_i+\beta_j X_j+2(\beta_i X_i)(\beta_j X_j)p+(\beta_i X_i)^2p+(\beta_j X_j)^2p}- \\ \dfrac{\beta_i X_i\varepsilon_i p_0}{1+\beta_i X_i p_0}\end{array}\right) \tag{B-9}$$

Assuming that permeability varies with porosity as Eq. (5), the permeability change can be effectively calculated as a function of elastic moduli, initial porosity and strain properties corresponding to single component gas behavior.

The input parameters for the model require separate absolute volumetric swelling experiments to be conducted on a coal sample for each gas component. These experiments will yield values for $\varepsilon_{i,j}$ and $P_{\Psi_{i,j}}$. All the input parameters required to model a differential swelling experiment were only available for Experiment V. The input parameters used are as follows:

ϕ_0 = 0.0194, [-]

k_0 = 2.309, mD

ν = 0.39, [-]

β_{CH_4} = 0.189, MPa^{-1}

β_{CO_2} = 0.33, MPa^{-1}

ε_{CH_4} = 0.0244, [-]

ε_{CO_2} = 0.042, [-]

$p_{initial}$ = 22.875, MPa

The model result for Experiment V is shown in Fig. 16. The model results match the experimental permeability values under unconstrained conditions. The model takes in as an input the change in the partial pressures of the individual components over the whole course of the experiment. The partial pressures were calculated from the measurements of the gas chromatograph. The composition of the produced gas is assumed to be the average composition of the free phase over the whole coal core. The fact that the CO_2 in the core moves with a distinct front cannot be ruled out.

NOMENCLATURE

H_v = enthalpy of vaporization, cal

δ = solubility parameter, $cal^{0.5}cm^{-1.5}$

V = molar volume, cm^3

M = constrained axial modulus, MPa

ν = poission ratio, [–]

ϕ = porosity, [–]

ϕ_0 = initial porosity, [–]

k = permeability, mD

k_0 = initial permeability, mD

γ = grain compressibility, MPa^{-1}

p = reservoir pressure, MPa

p_0 = initial reservoir pressure, MPa

$X_{i,j}$ = mole fraction, [–]

$p_{i,j}$ = partial pressure, MPa

$\beta_{i,j}$ = reciprocal of $P_{\Psi_{i,j}}$, MPa^{-1}

$P_{\Psi_{i,j}}$ = gas pressure at which the matrix strain is half the maximum value, MPa

$\varepsilon_{i,j}$ = maximum volumetric strain when the coal is fully saturated by a single gas component, [–]

q = flow rate $[m^3/\text{sec}]$,

P_0 = production pressure $[MPa]$,

P_i = injection pressure $[MPa]$,

μ = viscosity $[Pa.s]$,

A = crossection area $[cm^2]$

L = length of the core $[m]$

ACKNOWLEDGEMENTS

This work was funded by the EU funded CO_2 sequestration project "RECOPOL" and the Dutch "CATO" programme. At the very onset, we would like to thank Prof. Harpalani and Dr. Hans Bruning for their valuable input. They have been instrumental in solving our doubts, which have been basic at times. We would like to extend our gratitude once again to both of them for being patient, and inspiring us to walk on this path, which was arduous at times. My special thanks to Henk van Asten and Leo Vogt for their technical support. The experimental work would not have been possible without their help.

REFERENCES CITED

1. Arri, L. E., Yee, D., Morgan, W. D., Jeansonne, M. W. 1992: "Modelling coalbed methane production with binary gas sorption", SPE 24363, SPE Rocky Mountain Regional Meeting, Casper Wyoming.

2. Chikatamarla, L, Xiaojun, CUI and Bustin, R.M. 2004: "Implications of volumetric swelling / shrinkage of coal in sequestration of acid gases" International Coalbed Methane Symposium, May 3-7, Alabama, USA.

3. Durucan, S., Edwards, J. S. 1986: "The Effects of stress and fracturing on permeability of coal", Mining Science and Technology, Vol. 3, 205 -- 216.

4. Gilman, A., Beckie, R. 2000: "Flow of Coal-Bed Methane to a Gallery", Transport in Porous Media, 41, 1 -- 16.

5. Gray, I.: "Reservoir Engineering in coal Seams: Part 1-The physical process of gas storage and movement in coal seams", paper SPE 12514.

6. Hall, F. E., Chunhe, Z., Gasem, K. A. M., Robinson, R. L and Yee, D. 1994: "Adsorption of pure methane, nitrogen, and carbon dioxide and their binary mixtures on wet fruitland coal", SPE 29194, Eastern Regional Conference and Exhibition, Charleston, WV.

7. Harpalani, S., Zhao, X. 1989: "An investigation of the effect of gas desorption on coal permeability formation", Proc. Coalbed Methane Symposium, Tuscaloosa, Alabama, 57-64.

8. Holman, J. P. 1994: Experimental Methods for Engineers: 6th Edition McGraw - Hill Inc.

9. Kross, B. M., van Bergen, F., Gensterblum, Y., Siemons, N., Pagnier, H. J. M. and David, P. 2002: "High-pressure methane and carbon dioxide adsorption on dry and moisture-equilibrated Pennsylvanian coals", International Journal of Coal Geology, 51, 69-92.

10. Larsen, J. W. 2004: "The effects of dissolved CO_2 on coal structure and properties", International Journal of Coal Geology, 57, 63-70.

11. Levine, J.R.: "Model study of the influence of matrix shrinkage on absolute permeability of coal bed reservoirs", Coalbed Methane and Coal Geology, Geologic Society Special Publication, 109, 197-212.

12. Lucht, L. M. and Peppas, N. A. 1981: "New Approaches in Coal Chemistry", ACS Symposium Series, 43, 169.

13. Mavor, M. J., Gunter, W. D. 2004: "Secondary Porosity and Permeability of Coal vs. Gas Composition and Pressure", SPE 90255, SPE Annual Technical Conference and Exhibition, Houston, Texas.

14. Palmer, I, Mansoori, J. 1996: "How permeability depends on stress and pore pressure in coalbeds: A new Model", SPE 36737, Oct.

15. Pekot, L.J., Reeves, S.R. 2002: "Modelling coal matrix shrinkage and differential swelling with CO_2 Injection for enhanced coalbed methane recovery and carbon sequestration applications", Tropical Report, Advanced resources International, Texas, Nov.

16. Prusty, B. K., Harpalani, S. 2004: "A laboratory study of methane / CO_2 exchange in an enhanced CBM recovery Scenario", International Coalbed Methane Symposium, May 3-7, Alabama, USA.

17. Puri, R., Yee, D. 1990: "Enhanced coalbed methane recovery", SPE paper 20732, SPE 65th Annual Technical Conference and Exhibition, New Orleans, Louisiana.

18. Reucroft, P. J. & Patel, H. 1986: "Gas induced swelling in Coal", Fuel, 65, 816 -- 820.

19. Sawyer, W. K., Paul, G. W., and Schraufnagel, R. A. 1990: "Development and Application of a 3D Coalbed Simulator", Paper CIM / SPE, Proc. Petroleum Society CIM, Calgary, 90 -- 119.

20. Seidle, J.P., et al. 1995: "Experimental Measurement of Coal Matrix Shrinkage due to gas desorption and implications for cleat permeability increases", paper SPE 30010.

21. Shi, J.Q & Durucan, S. 2003: "Changes in permeability of coalbeds during primary recovery", International Coalbed Methane Symposium, May 5-9, Alabama, USA.

22. Somerton, W., et al. 1975: "Effect of stress on permeability of coal", International Journal of Rock Mechanics and Mining Sciences, vol. 12, 129 -- 145.

23. Taylor, J. R. 1997: An Introduction to Error Analysis: 2^{nd} Edition University Science Books, Sausalito, California.

24. Zutshi, A & Harpalani, S. 2004: "Matrix Swelling with CO_2 Injection in CBM Reservoirs and its Impact on Permeability of Coal", International Coalbed Methane Symposium, May 3-7, Alabama, USA.

Sample	Rank [% R_{max}]	Maceral composition [%]		Specific surface [m^2/g]	Micropore volume [cm^3/g coal]
Beringen 770 (Belgium)	0.78	Vitrinite	37.8	151.53	0.055
		Liptinite	18.0		
		Inertinite	44.0		
		Mineral matter	0.2		
Silezia 315 II (Poland)	0.68	Vitrinite	71.6	190.00	0.064
		Liptinite	6.8		
		Inertinite	15.0		
		Mineral matter	6.8		
Tupton (UK)	0.53	Vitrinite	59.4	244.10	0.08294
		Liptinite	14.0		
		Inertinite	25.8		
		Mineral matter	0.8		

Table 1. Compositional and structural details of the coal samples used for the differential sorption experiments

Experiment	Length [mm]	Diameter [mm]	P_{mean} [MPa]	P_{eff} [MPa]	Injection rate [ml/hr]	Free CH_4 [moles]	Adsorbed CH_4 [moles]
I (Beringen 770)	334.00	69.50	4.3	3.61	6	0.43	0.61
II (Beringen 770)	178.30	69.50	8.12	2.01	0.7	0.402	0.83
III (Silezia 315 II)	200.50	69.50	8.325	2.25	1	0.1337	0.2913
IV (Silezia 315 II)	200.50	69.50	9.08	1.59	1	0.5176	0.409
V (Tupton)	227.00	75.00	22.85	3.195	1	1.5672	0.4318

Table 2. Details of the coal cores used for the differential sorption experiments, the experimental conditions, injection rates and methane saturation

CO_2 flooding (Beringen 770)	CO_2 = 1 %		CO_2 = 50 %		CO_2 = 90 %	
	Dry (6ml/hr)	Dry (0.7ml/hr)	Dry (6ml/hr)	Dry (0.7ml/hr)	Dry (6ml/hr)	Dry (0.7ml/hr)
Sweep efficiency [%]	43.6	22.9	58.8	46.7	69.1	58.7
Displaced volume [mole/mole]	0.91	1.77	1.36	5.1	2.06	10.63
Time after production [sec]	3.36×10^5	6.6×10^5	5.0×10^5	19.0×10^5	7.7×10^5	39.6×10^5

Table 3. Sweep efficiency, displaced volume and time of experiment I and II

CO_2 flooding (Silesia 315 II)	CO_2 = 1 %		CO_2 = 50 %		CO_2 = 90 %	
	Dry	Wet	Dry	Wet	Dry	Wet
Sweep efficiency [%]	37.2	11.6	66.25	16.5	69.8	19.5
Displaced volume [mole/mole]	1.28	1.26	2.56	2.09	2.96	2.86
Time after production [sec]	3.8×10^5	2.7×10^5	7.6×10^5	4.5×10^5	8.8×10^5	6.1×10^5

Table 4. Sweep efficiency, displaced volume and time of experiment III and IV

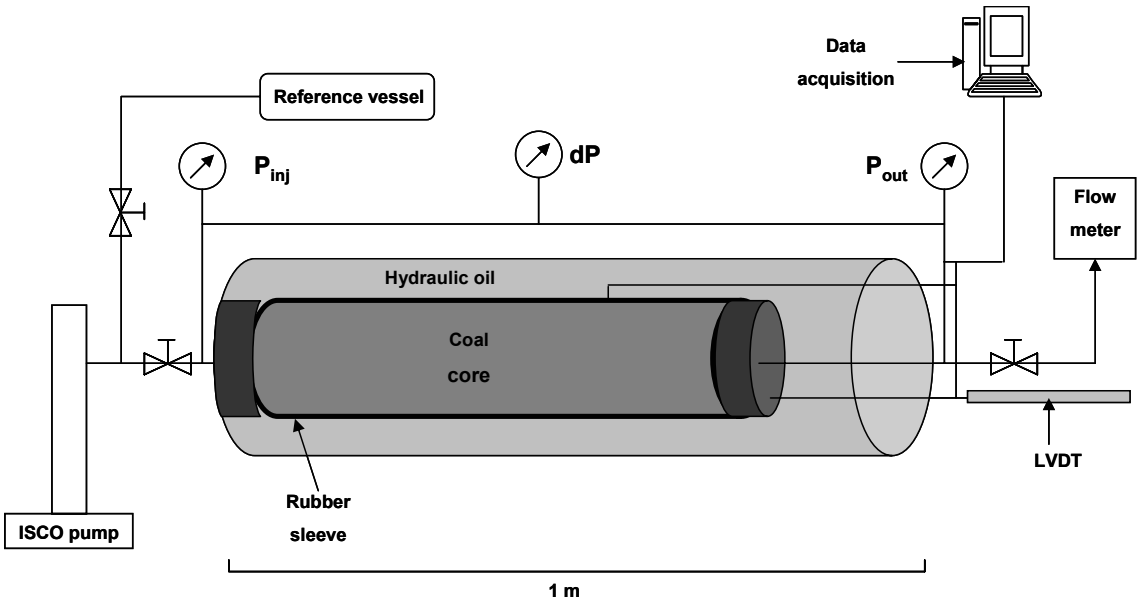

Figure 1 Schematic of the high pressure flow cell

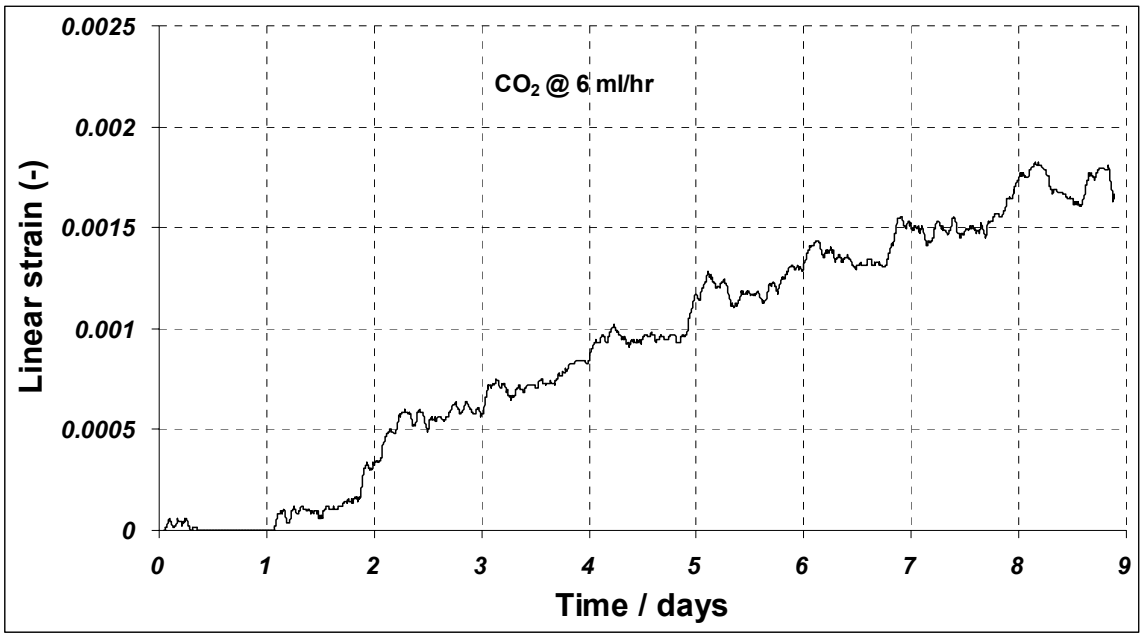

Figure 2 Differential swelling measured as linear strain of the Beringen 770 from Experiment I

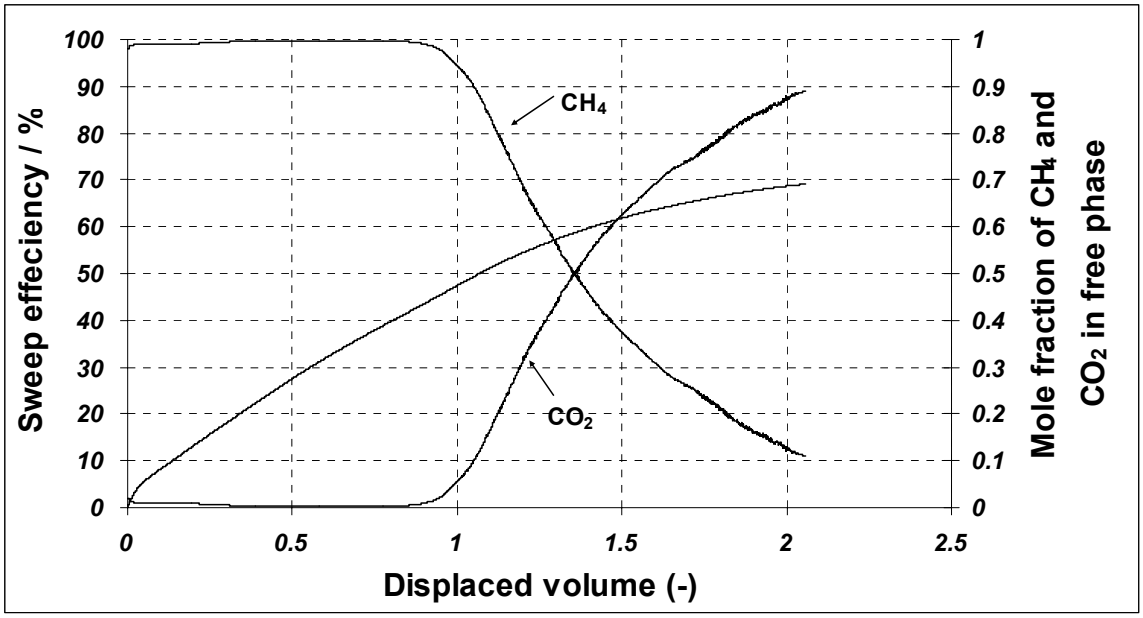

Figure 3 Sweep efficiency and molar concentrations of the produced gas against displaced volume from Experiment I

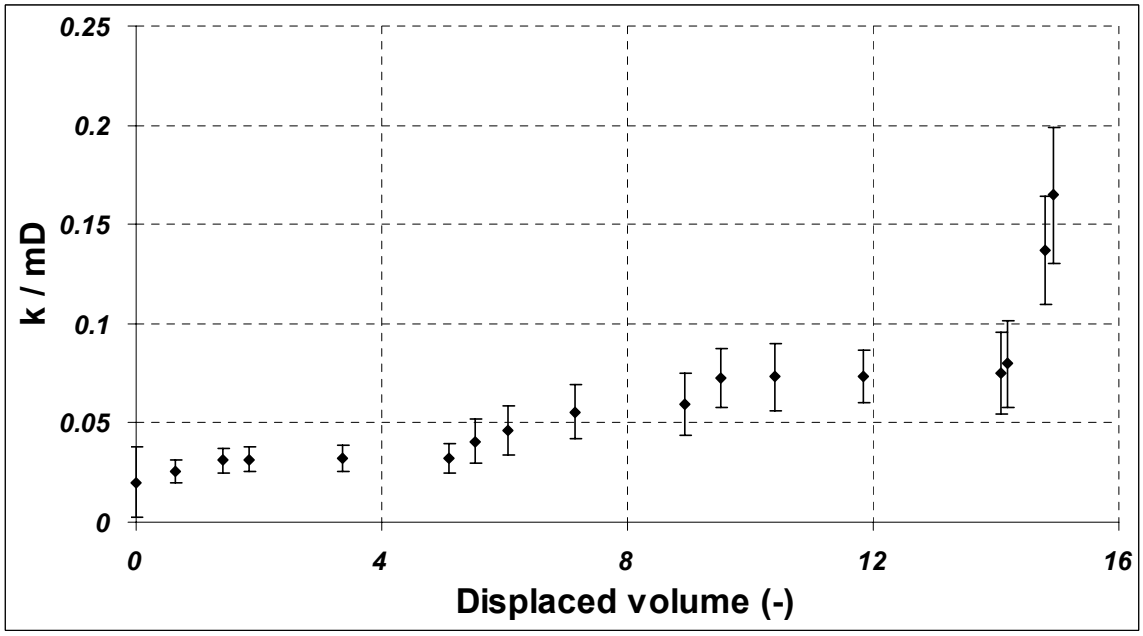

Figure 4 Experimentally determined variation in permeability for the Beringen 770 coal as a result of differential swelling from Experiment II under unconstrained conditions

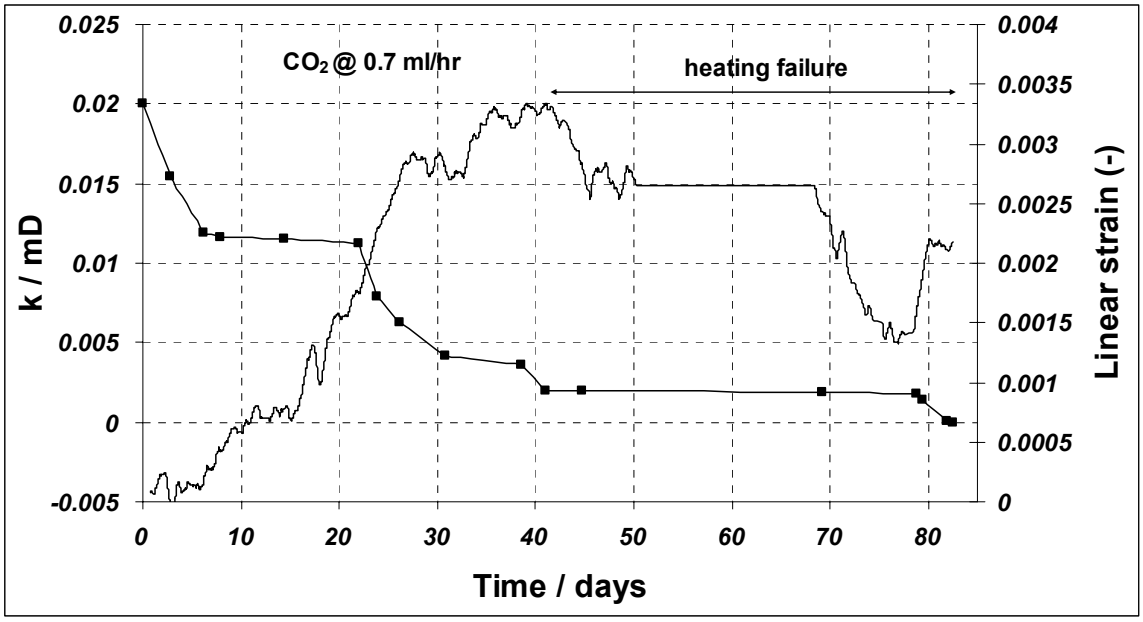

Figure 5 Estimated permeability variations for Beringen 770 under constrained conditions using experimentally determined permeability data from Experiment II

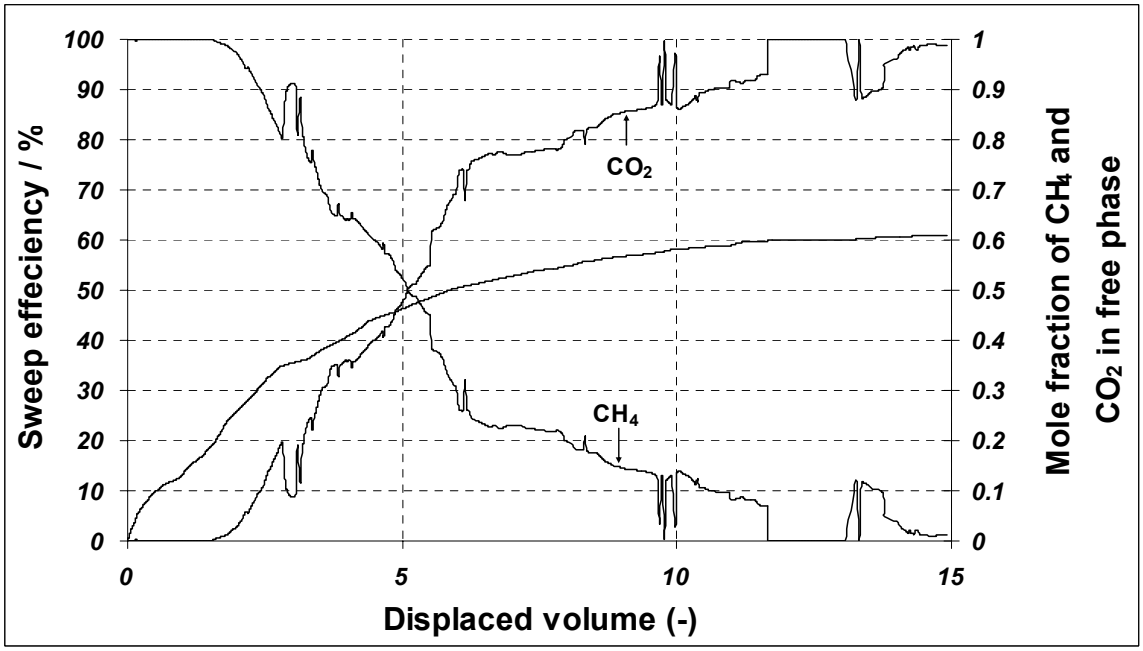

Figure 6 Sweep efficiency and molar concentrations of the produced gas against displaced volume from Experiment II

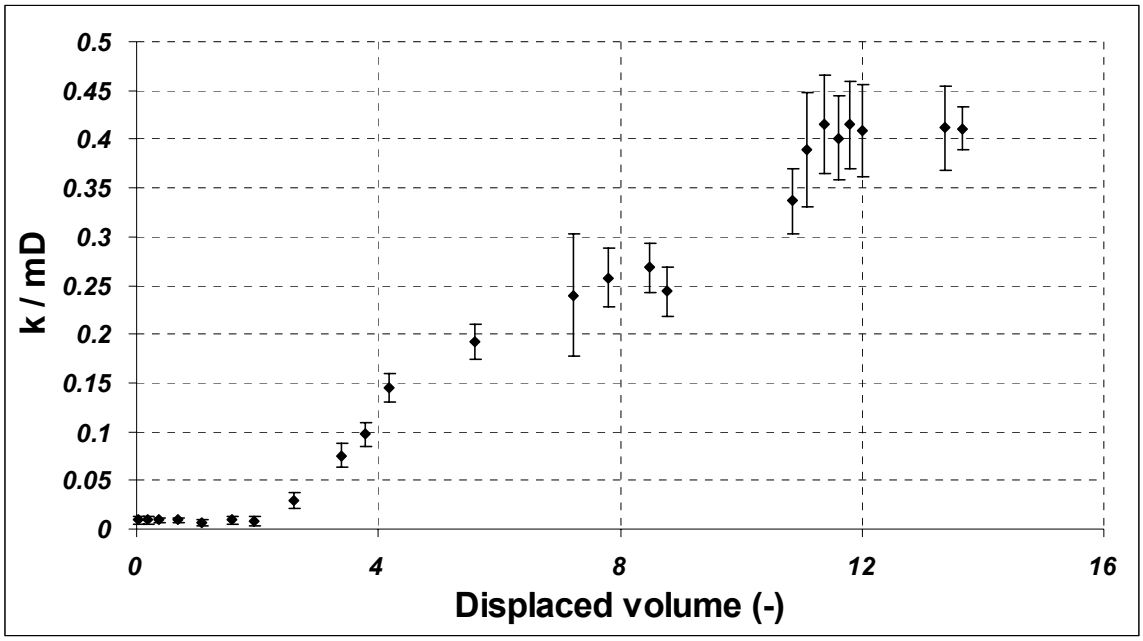

Figure 7 Experimentally determined variation in permeability for a moist Silezia 315 II coal as a result of differential swelling from Experiment III under unconstrained conditions

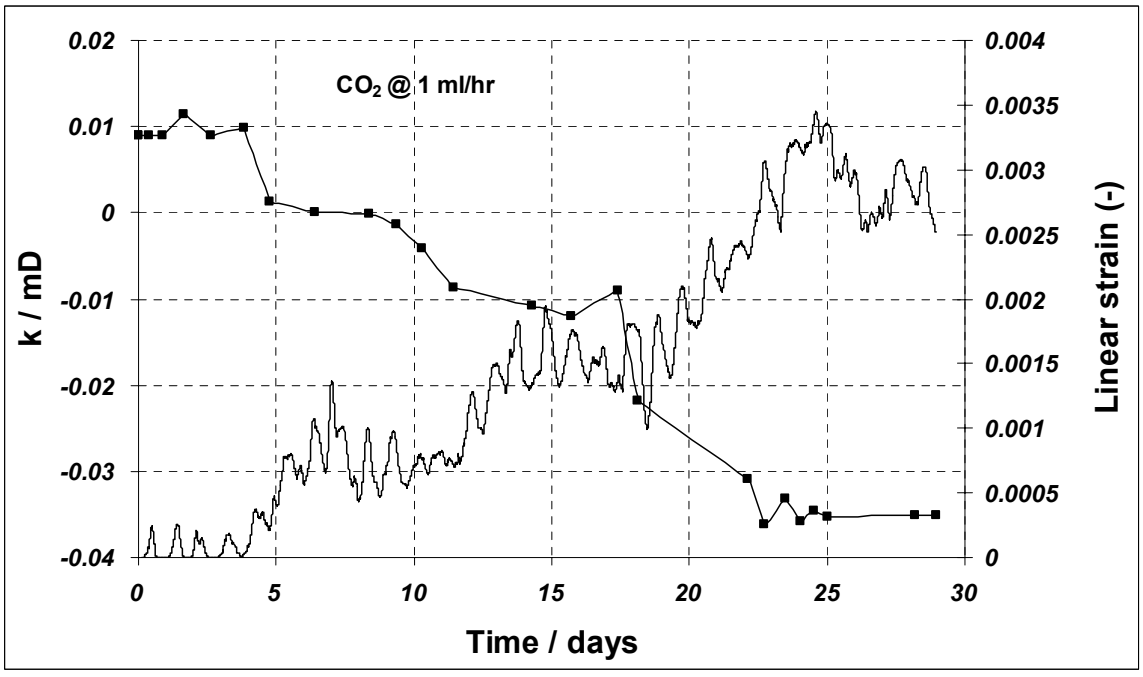

Figure 8 Estimated permeability variation for Silezia 315 II under constrained conditions using experimentally determined permeability data from Experiment III

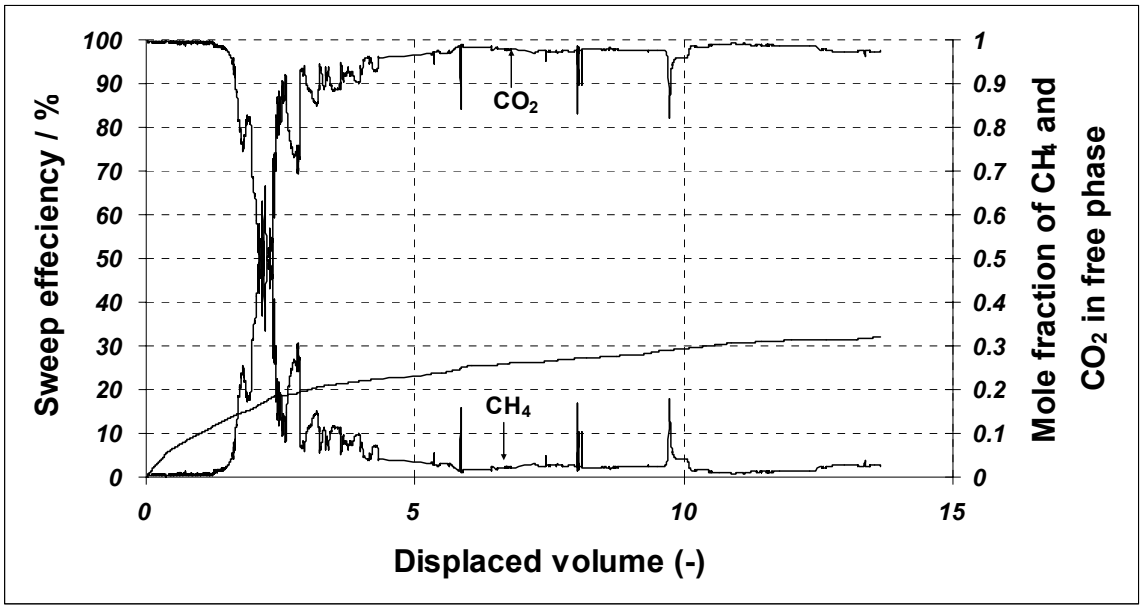

Figure 9 Sweep efficiency and molar concentration of the produced gas against displaced volume from Experiment III

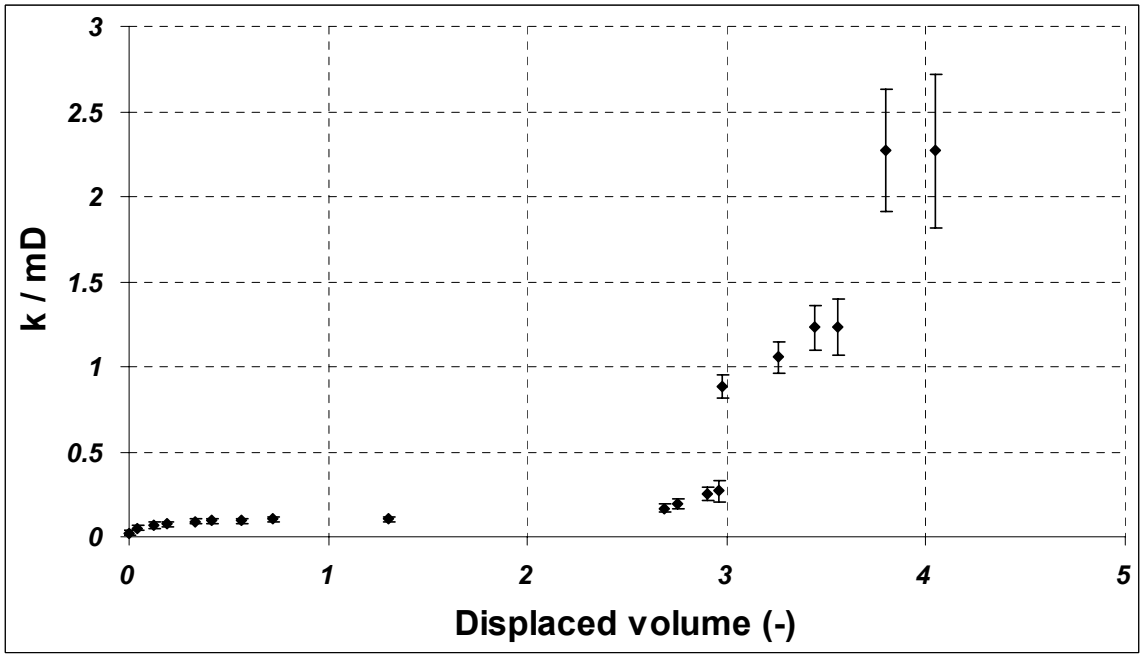

Figure 10 Experimentally determined variation in permeability for the dry Silezia 315 II coal as a result of differential swelling from Experiment IV under unconstrained conditions

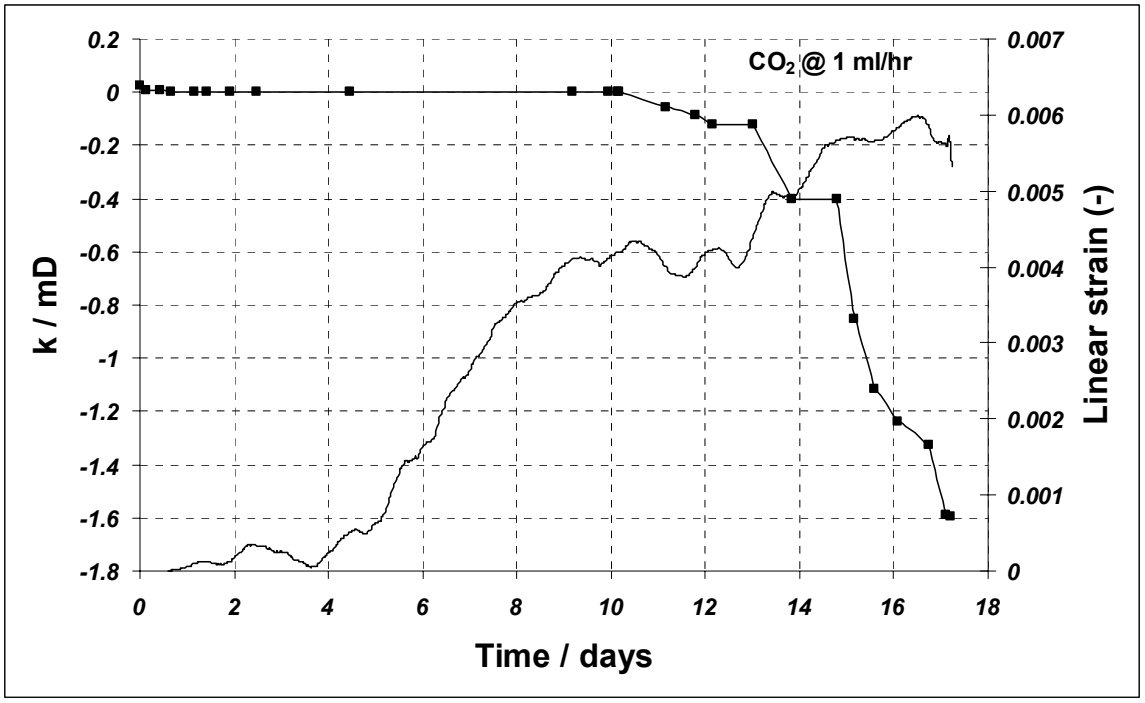

Figure 11 Estimated permeability variation for dry Silezia 315 II under constrained conditions using experimentally determined permeability data from Experiment IV

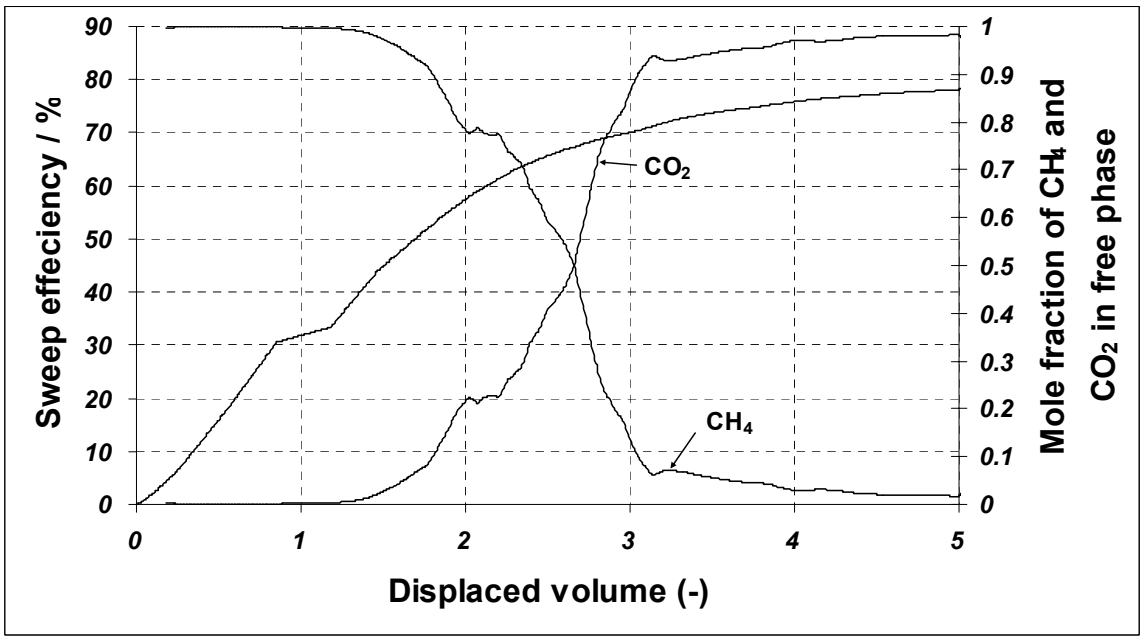

Figure 12 Sweep efficiency and molar concentrations of the produced gas against displaced volume from Experiment IV

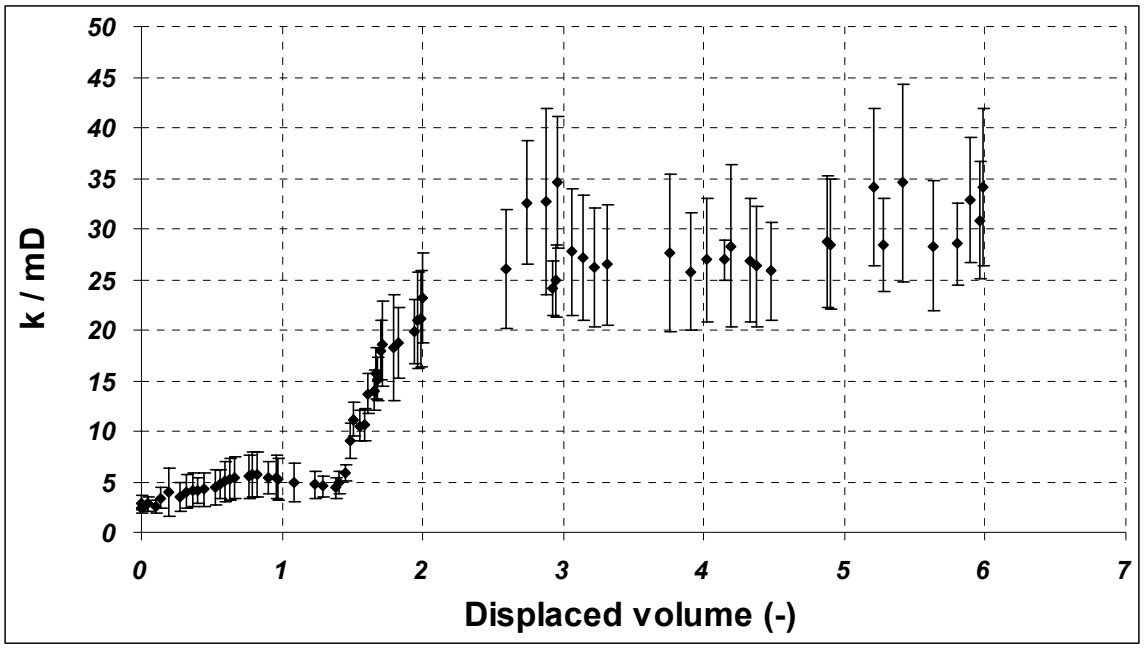

Figure 13 Experimentally determined variation in permeability for the dry Tupton coal as a result of differential swelling from Experiment V under unconstrained conditions

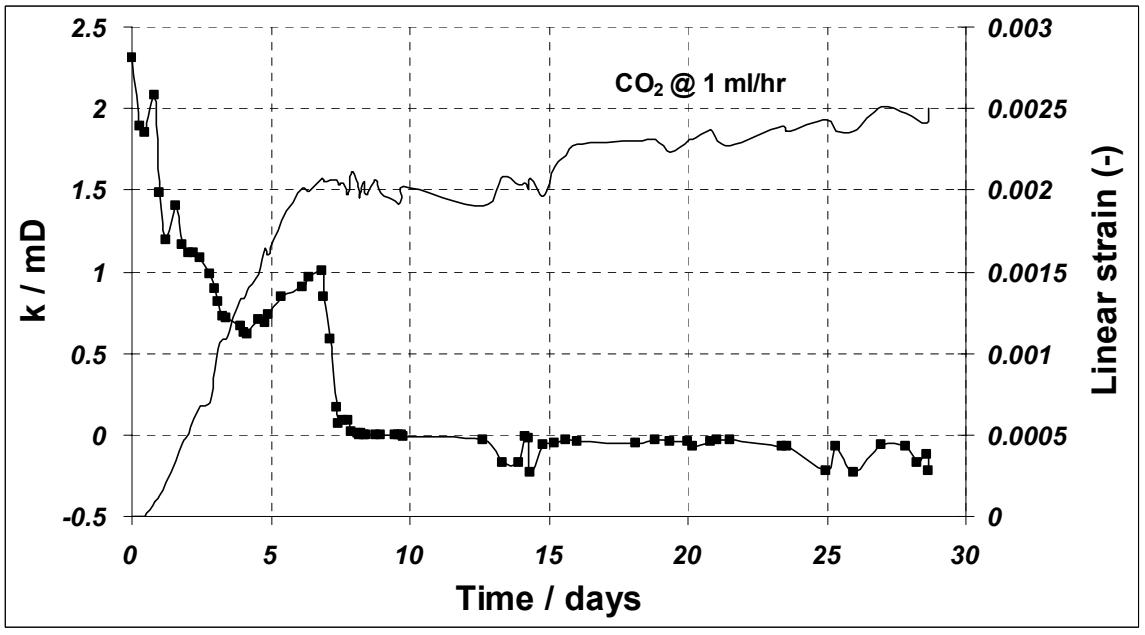

Figure 14 Estimated permeability variation for dry Tupton under constrained conditions using experimentally determined permeability data from Experiment V

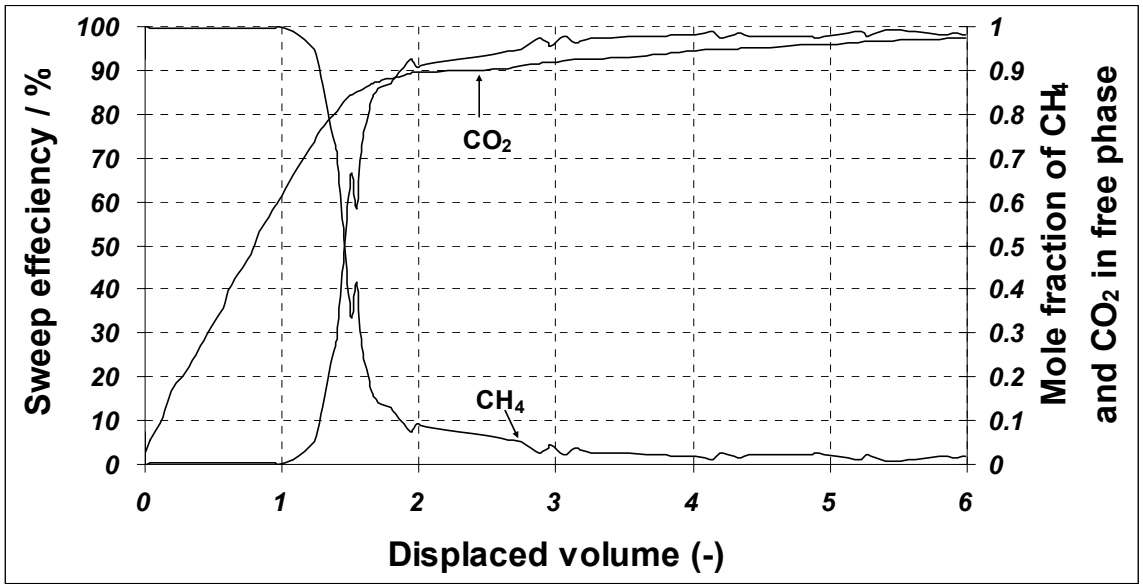

Figure 15 Sweep efficiency and molar concentrations of the produced gas against displaced volume from Experiment V

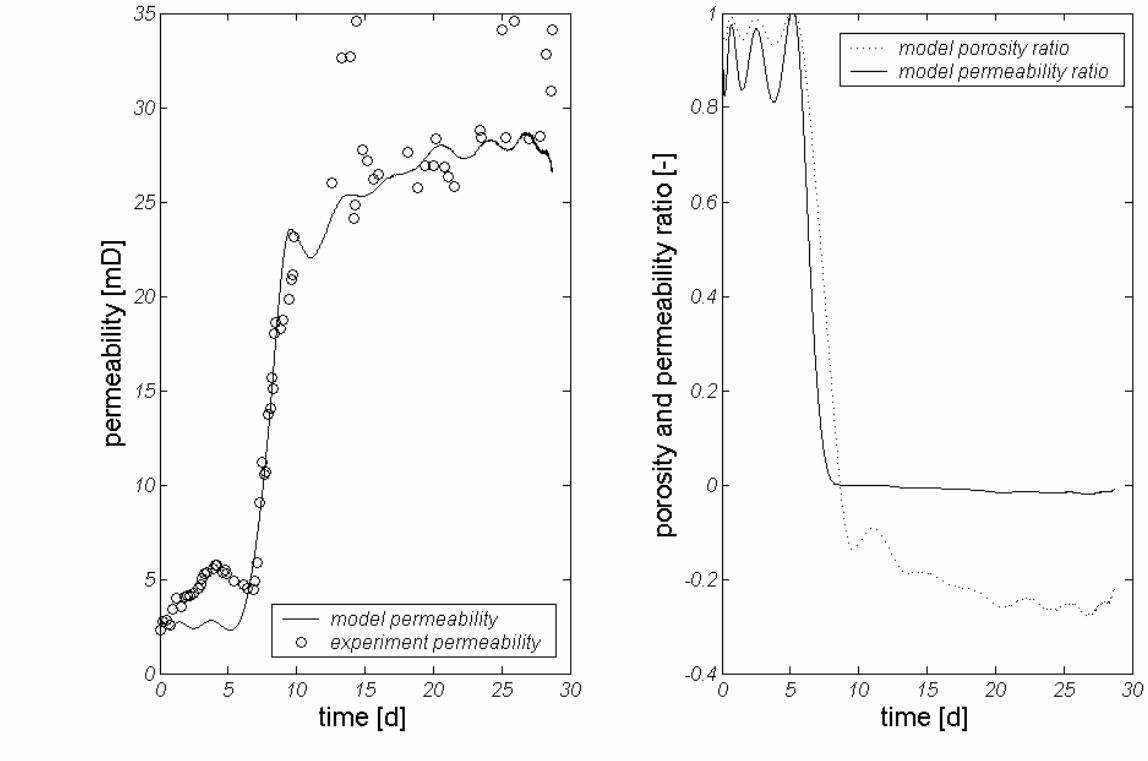

Figure 16 Model results predicting the permeability variation corresponding to the differential swelling of Tupton coal from Experiment V under both unconstrained and constrained conditions